Minimal Determinants for Binding Activated Gα from the Structure of a $G\alpha_{i1}$−Peptide Dimer[†,‡]

Christopher A. Johnston,[§] Ekaterina S. Lobanova,[∥] Alexander S. Shavkunov,[∥] Justin Low,[⊥] J. Kevin Ramer,[@,#] Rainer Blaesius,[@,+] Zoey Fredericks,[@,○] Francis S. Willard,[§] Brian Kuhlman,[⊥] Vadim Y. Arshavsky,[∥] and David P. Siderovski*[,§]

Departments of Pharmacology and of Biochemistry and Biophysics, University of North Carolina School of Medicine, Chapel Hill, North Carolina 27599-7365, Departments of Ophthalmology and Neurobiology, Duke University, Durham, North Carolina 27710, and Karo Bio USA, Durham, North Carolina 27703

Received July 8, 2006; Revised Manuscript Received July 27, 2006

ABSTRACT: G-Proteins cycle between an inactive GDP-bound state and an active GTP-bound state, serving as molecular switches that coordinate cellular signaling. We recently used phage display to identify a series of peptides that bind Gα subunits in a nucleotide-dependent manner [Johnston, C. A., Willard, F. S., Jezyk, M. R., Fredericks, Z., Bodor, E. T., Jones, M. B., Blaesius, R., Watts, V. J., Harden, T. K., Sondek, J., Ramer, J. K., and Siderovski, D. P. (2005) *Structure 13*, 1069−1080]. Here we describe the structural features and functions of KB-1753, a peptide that binds selectively to GDP·AlF_4^-- and GTPγS-bound states of $G\alpha_i$ subunits. KB-1753 blocks interaction of $G\alpha_{transducin}$ with its effector, cGMP phosphodiesterase, and inhibits transducin-mediated activation of cGMP degradation. Additionally, KB-1753 interferes with RGS protein binding and resultant GAP activity. A fluorescent KB-1753 variant was found to act as a sensor for activated Gα in vitro. The crystal structure of KB-1753 bound to $G\alpha_{i1}$·GDP·AlF_4^- reveals binding to a conserved hydrophobic groove between switch II and α3 helices and, along with supporting biochemical data and previous structural analyses, supports the notion that this is the site of effector interactions for $G\alpha_i$ subunits.

Heterotrimeric G-proteins serve as critical relays that transmit cues from extracellular stimuli as diverse as neurotransmitters, hormones, photons, and odorants/tastants to intracellular signaling cascades responsible for eliciting specific cellular effects (*1*, *2*). In the traditional model of G-protein signaling, cell surface G-protein-coupled receptors (GPCRs),[1] upon activation by the aforementioned stimuli, catalyze the exchange of GDP for GTP on the Gα subunit. This results in adoption of the active, GTP-bound Gα conformation, which dissociates from the Gβγ dimer formerly bound to inactive Gα·GDP as a heterotrimeric Gαβγ complex. Gα·GTP and freed Gβγ then regulate a variety of downstream effectors by both individual and coordinated mechanisms (*1*, *2*). The GTP-dependent conformational changes within Gα required for effector binding are known for $G\alpha_s$ bound to adenylyl cyclase (*3*), $G\alpha_{transducin}$ ($G\alpha_t$) bound to the γ-subunit of cGMP phosphodiesterase (PDEγ) (*4*), $G\alpha_{13}$ bound to p115RhoGEF (*5*), and $G\alpha_q$ bound to GRK2 (*6*). However, no effector-bound structure of $G\alpha_{i1-3}$ has yet been determined. Signaling of Gα·GTP to effectors is terminated by the intrinsic GTP hydrolysis activity of Gα, returning it to the GDP-bound conformation and Gβγ reassociation. GTP hydrolysis can be dramatically enhanced by the family of proteins known as "regulators of G-protein signaling" (RGS), which serve as GTPase-accelerating proteins (GAPs) for Gα subunits (*7*, *8*). This model of nucleotide cycling predicts that the duration and intensity of signaling are ultimately determined by the lifetime of Gα in the activated, GTP-bound conformation. Therefore, a complete understanding of the molecular determinants of the guanine nucleotide cycle is of particular importance in understanding the temporal aspects governing G-protein-mediated signal transduction.

[†] This work was supported by NIH Grants R01 GM074268 (D.P.S.) and EY12859 (V.Y.A.). C.A.J. was supported by a NIH postdoctoral fellowship (1 F32 GM076944). V.Y.A. is the recipient of the Senior Scientific Investigator Award from Research to Prevent Blindness Inc.

[‡] Coordinates of the KB-1753−$G\alpha_{i1}$·GDP·AlF_4^- complex were deposited in the Protein Data Bank as entry 2G83.

* To whom correspondence should be addressed: Department of Pharmacology, University of North Carolina School of Medicine, 1106 M.E. Jones Bldg., Chapel Hill, NC 27599-7365. Telephone: (919) 843-9363. Fax: (919) 966-5640. E-mail: dsiderov@med.unc.edu.

[§] Department of Pharmacology, University of North Carolina School of Medicine.

[∥] Duke University.

[⊥] Department of Biochemistry and Biophysics, University of North Carolina School of Medicine.

[@] Karo Bio USA.

[#] Current address: Entegrion, 5312 Farrington Rd., Chapel Hill, NC 27517.

[+] Current address: Becton Dickinson, 21 Davis Dr., Research Triangle Park, NC 27709.

[○] Current address: Amgen Inc., 1201 Amgen Court W., Seattle, WA 98119.

[1] Abbreviations: AlF_4^-, aluminum tetrafluoride; CFP, cyan fluorescent protein; cGMP, cyclic guanosine monophosphate; FRET, fluorescence resonance energy transfer; GAP, GTPase-accelerating protein; GDP, guanosine diphosphate; GEF, guanine nucleotide exchange factor; GMP, guanosine monophosphate; GPCR, G-protein-coupled receptor; GTP, guanosine triphosphate; PDE, phosphodiesterase; RGS, regulator of G-protein signaling; ROS, rod outer segment; SPR, surface plasmon resonance; YFP, yellow fluorescent protein.

10.1021/bi0613832 CCC: $33.50
Published on Web 08/30/2006

We recently employed phage display technology to identify peptides capable of interacting with Gα in a conformation-dependent manner (*9*, *10*). These peptides selectively bind Gα by distinguishing key structural orientations of the critical "switch regions" in Gα that govern nucleotide exchange and hydrolysis and control interaction with regulatory proteins and effectors (*11*). In addition to their discriminatory binding properties, these peptides can possess intrinsic regulatory properties that provide insight into the regulation of Gα signaling. For example, we recently described the molecular basis for the interaction of a GDP-selective peptide, KB-752, with Gα·GDP (*10*). KB-752 serves as a guanine nucleotide exchange factor (GEF) in vitro, and the structure of the Gα−KB-752 complex provided insight into the role of switch II displacement in the mechanism of GPCR-mediated nucleotide exchange, a process that remains largely elusive (*12*−*14*). Several other groups have also used similar techniques to identify Gα- and Gβγ-binding peptides that have provided insight with regard to the mechanics of heterotrimeric G-protein signaling (*15*−*18*).

Here we describe the crystal structure of a peptide, KB-1753, that interacts exclusively with activated $G\alpha_i$ subunits, including the closely related $G\alpha_{transducin}$. The structure of the KB-1753−$G\alpha_{i1}$·GDP·AlF_4^- complex reveals the molecular determinants of nucleotide-selective binding of KB-1753 to Gα, highlighting the importance of the disposition of the switch II helix. KB-1753 competitively antagonizes the binding of PDEγ to $G\alpha_t$, suggesting that KB-1753 binds in a fashion similar to that of effectors. Additionally, KB-1753 prevents RGS protein binding and resultant GAP activity toward $G\alpha_{i1}$ and $G\alpha_t$. We also demonstrate the utility of a fluorescently modified KB-1753 to serve as a sensor for activated $G\alpha_{i1}$ in vitro. Collectively, our results represent the first structure of $G\alpha_{i1}$ engaging an activation-state-selective target in its effector-binding region and underscore the usefulness of the KB-1753 peptide as a tool for studying G-protein signal transduction.

MATERIALS AND METHODS

Materials. Unless noted, all reagents were from Sigma. Peptides were synthesized by Anaspec (San Jose, CA), except for the C-terminal cysteine variant of KB-1753 and PDEγ-(63−87) (GLGTDITVICPWEAFNHLELHELAQYGII), which were synthesized by the Tufts University Core Facility (directed by M. Berne).

KB-1753/YFP Plasmid Construction. Oligonucleotides encoding KB-1753 were constructed with 5′-*Kpn*I and 3′-*Bam*HI overhangs: sense, 5′-CGT CTT CTC GAG GTT ACT ACC ATG GTA TTT GGG TGG GTG AAG AAG GTC GAC TTT CTC GAT GC-3′; and antisense, 5′-GAT CGC ATC GAG AAA GTC GAC CTT CTT CAC CCA CCC AAA TAC CAT GGT AGT AAC CTC GAG AAG ACG GTA C-3′; 100 ng of each primer were mixed, denatured, annealed (55 °C for 1 min), and cooled prior to ligation into *Kpn*I- and *Bam*HI-digested pEYFP-N1 (Clontech). To avoid steric hindrance of the KB-1753−Gα interaction by YFP, we inserted a flexible linker (Gly-Ser-Gly-Gly-Ser-Gly) between KB-1753 and YFP by insertional mutagenesis (QuickChange, Stratagene) with the following primers: sense, 5′-CGA CTT TCT CGA TGC GGA TCT GGT GGC TCA GGG GAT CCA CCG GTC GCC-3′; and antisense, 5′-GGC GAC CGG TGG ATC CCC TGA GCC ACC AGA TCC GCA TCG AGA AAG TCG-3′. The KB-1753−linker−YFP open reading frame was then isolated using PCR [30 cycles of 95 °C denaturing (30 s), 55 °C annealing (1 min), and 72 °C extension (1 min)] using primers (sense, 5′-TAC TTC CAA TCC AAT GCG TCT TCT CGA GGT TAC TAC CAT GGT ATT-3′; and antisense, 5′-TTA TCC ACT TCC AAT GCG CTA CTT GTA CAG CTC GTC CAT GCC GAG AGT-3′) and then subcloned into an N-terminal His_6-tagged vector using a ligation-independent strategy described previously (*19*).

Protein Production. His_6-tagged N-terminally truncated human $G\alpha_{i1}$ (ΔN-$G\alpha_{i1}$), as well as full-length $G\alpha_{i2}$, $G\alpha_{i3}$, and $G\alpha_{oA}$ subunits, was purified from *Escherichia coli* as previously described (*20*, *21*). The His_6-tagged RGS12 RGS domain (amino acids 702−846 of SwissProt entry O08774) was cloned into pMCSG7 using a ligation-independent cloning strategy (*19*) and purified as described for $G\alpha_{i1}$. His_6-tagged human RGS16 (amino acids 53−190; ref *22*) was prepared from the expression construct pLIC-SGC1-RGS16-s001 obtained from SGC (Oxford), per their published protocol (PDB entry 2BT2). Transducin heterotrimer and PDE6 were purified from bovine retinas as described previously (*23*); urea-treated photoreceptor membranes used as the source of photoactivated rhodopsin were purified from bovine retinas as previously described (*24*).

Surface Plasmon Resonance. SPR binding assays were performed at 25 °C using a BIAcore 3000 instrument. N-Terminally biotinylated KB-1753 or PDEγ(63−87) peptides {diluted to 0.1 μg/mL in BIA-run buffer [10 mM HEPES (pH 7.4), 150 mM NaCl, 10 mM $MgCl_2$, and 0.005% NP40]} were coupled to flow cells of streptavidin biosensors (Biacore) to a surface density of ∼500 RU. Gα subunits were diluted in BIA-run buffer in the presence of 100 μM GDP, 100 μM GDP with 30 μM $AlCl_3$ and 10 mM NaF, or 100 μM GTPγS and incubated at room temperature for 2 h. Gα subunits in desired nucleotide states (30 μL) were then injected over flow cells at 10 μL/min, followed by a 300 s dissociation phase. To correct for nonspecific binding and buffer shift artifacts, binding curves from a surface containing a control peptide (mNOTCH1; ref *25*) were subtracted from all binding curves. Surfaces were regenerated with two 10 μL injections of 500 mM NaCl with 25 mM NaOH at 20 μL/min. BIAevaluation version 3.0 was used for binding curve and kinetic analyses. Dissociation constants (K_D) were determined by saturation binding as previously described (*20*, *21*).

Crystallization and Structure Determination. ΔN-$G\alpha_{i1}$ protein [25 mg/mL in 20 mM Tris (pH 7.5), 1 mM $MgCl_2$, 20 mM NaCl, 1 mM DTT, 5% glycerol, 10 μM GDP, 30 μM $AlCl_3$, and 10 mM NaF] was incubated with a 1.5-fold molar excess of KB-1753 at room temperature for 5 min prior to screening. Initial crystals were obtained in condition 28 of the PEG-Ion Screen (Hampton Research) and refined to final crystallization conditions of 15% PEG-8000 and 0.3 M calcium acetate using the vapor diffusion method with 8 μL hanging drops with a 1:1 protein:buffer volume ratio. Crystals formed in 2−4 days at 4 °C in space group $P3_221$ ($a = b = 103.13$ Å, $c = 206.99$ Å, $\alpha = \beta = 90°$, and $\gamma = 120°$) with two $G\alpha_{i1}$−KB-1753 heterodimers in the asymmetric unit. Crystals were cryoprotected in crystallization

buffer supplemented with 20% glycerol for ~1 min and then submerged in liquid N_2. A 2.8 Å native data set was collected at Brookhaven National Laboratory using the x29 beamline. Data were scaled and indexed using HKL2000 (*26*). The structure of $G\alpha_{i1}$·GDP·AlF_4^- (PDB entry 1GFI), excluding waters, GDP, and AlF_4^-, was used for molecular replacement (*27*). Initial solutions were found with correlation coefficients of 57.5 and a starting *R*-factor of 47.6, which was reduced to 39.7 with an initial round of refinement. Model building was completed using O (*28*), with successive rounds of simulated annealing, minimization, and B-group and rigid body refinements being completed by CNS (*29*). Noncrystallographic symmetry restraints were used in initial cycles of refinement, and both $G\alpha_{i1}$−KB-1753 dimers were essentially identical. All electron density map calculations were completed with CNS. N-Terminal residues 25−32 of $G\alpha_{i1}$ were disordered along with residues 112−121 in the αB−αC loop of the all-helical domain; these segments were excluded in the final $G\alpha_{i1}$−KB-1753 model. All structural images were generated using PyMol (DeLano Scientific, San Carlos, CA).

PDE6 Activity Assays. PDE6 activity was measured as described previously (*30*). Briefly, illuminated urea-treated photoreceptor membranes (20 μL; final rhodopsin concentration of 10 μM), a source of photoexcited rhodopsin, were reconstituted with purified transducin (1 μM) at room temperature in buffer containing 10 μL of GTPγS, 100 mM NaCl, 8 mM $MgCl_2$, and 10 mM Tris-HCl (pH 7.8). When needed, 20 μM wild-type or mutant KB-1753 peptide was also added. PDE6 (0.05 μM) was added immediately before the reaction was initiated by addition of 10 μL of [^{3}H]cGMP (2.5 mM containing ~10^5 dpm/sample) and terminated by addition of 100 μL of 0.1 M HCl. The mixture was then neutralized with 100 μL of 0.1 M Tris and incubated with 75 μL of king cobra snake venom (1 mg/mL) for 1 h to convert GMP to guanosine. The solution was then passed through an anion exchange DEAE-Sepharose column to separate guanosine from cGMP and washed twice with 0.8 mL of H_2O. The eluent was mixed with 10 mL of ScintiSafe cocktail, and radioactivity was measured by scintillation counting.

GTPase Assays. Single-turnover GTPase assays with $G\alpha_{i1}$ were conducted as described previously (*31*). Briefly, 100 nM $G\alpha_{i1}$ was incubated at 30 °C for 15 min in buffer C [50 mM Tris (pH 7.5), 0.05% $C_{12}E_{10}$, 1 mM DTT, 5 μg/mL BSA, 10 mM EDTA, and 100 mM NaCl] containing ~1×10^6 cpm of [γ-^{32}P]GTP (6000 Ci/mmol). Samples were then placed on ice for 5 min. Reactions (on ice) were initiated by adding 10 mM $MgCl_2$ (with 100 μM GTPγS), and timed reaction aliquots were quenched with a charcoal slurry [containing 20 mM H_3PO_4 (pH 3)] followed by centrifugation (~4000*g* for 10 min at 4 °C). Supernatants with free γ-$^{32}P_i$ were analyzed by scintillation counting. Background counts (in the absence of $G\alpha_{i1}$) were subtracted from all experimental conditions.

Multiple-turnover GTPase assays with $G\alpha_t$ were conducted as described previously (*32*). Briefly, illuminated urea-treated photoreceptor membranes were mixed with transducin at room temperature in a buffer containing 100 mM NaCl, 8 mM $MgCl_2$, 10 mM Tris·HCl (pH 7.8), and 1 mM DTT. The reaction was started by the addition of 10 μL of [γ-^{32}P]-GTP at a desired concentration (final concentration of 20 μM; approximately 10^5 dpm/sample) to 20 μL of membranes (final concentrations of 10 μM rhodopsin and 1 μM transducin) supplemented with additional proteins and/or peptides when needed. The reaction was stopped by 100 μL of 6% perchloric acid. $^{32}P_i$ formation was assessed with activated charcoal. In the experiment addressing the effect of PDEγ on RGS16 GAP activity, the PDEγ(63−87) peptide was used instead of full-length PDEγ because this peptide completely substitutes for PDEγ in RGS protein regulation but, unlike PDEγ, does not block repetitive transducin activation by rhodopsin (*33*).

Fluorescence Resonance Energy Transfer (FRET) Assays. FRET assays for Gα−RGS interaction, along with purification of $G\alpha_{i1}$−CFP and YFP−RGS4, were completed as described previously (*34*). $G\alpha_{i1}$−CFP was diluted in 10 mM Tris (pH 8.0), 1 mM EDTA, 10 mM $MgCl_2$, 150 mM NaCl, and 10 μM GDP. Experiments on the effects of AlF_4^- activation were performed in buffer supplemented with 30 μM $AlCl_3$ and 10 mM NaF. Measurements were taken with a LS-55B spectrofluorimeter (Perkin-Elmer). Emission scans were performed at 20 nm/min using excitation of 433 nm, with slit widths of 5 nm. Emission maxima used for CFP and YFP were 474 and 525 nm, respectively. For peptide competition experiments, $G\alpha_{i1}$ (200 nM) was allowed to incubate in the quartz cuvette with wild-type or mutant KB-1753 (2 μM) for 2 min prior to addition of YFP−RGS4.

RESULTS

Identification of an Activated-State-Selective Gα Binding Peptide. To identify peptides capable of interacting with Gα selectively in the activated conformation, we performed phage display analysis as previously described for peptides that bind inactivated, GDP-bound Gα (*9*, *10*). Of the GTPγS-dependent $G\alpha_{i1}$ binding peptides that were obtained, seven peptides shared a consensus sequence of three hydrophobic residues centered around tryptophan and flanked by glycines (Figure 1A). A MOTIF search (http://motif.genome.jp/) of the Swiss-Prot protein database (*35*) with the degenerate sequence motif G-[IV]-W-[ILMSVW]-G revealed 166 proteins bearing this peptide signature across all represented genomes, but none was a known G-protein effector (data not shown). From this family of seven peptides, the longest and most avid binder, KB-1753, became the focus of our current efforts. To quantitate the nucleotide-dependent interaction of KB-1753 with $G\alpha_{i1}$, we performed surface plasmon resonance (SPR) measurements on a streptavidin biosensor coated with biotinylated KB-1753. Injection of $G\alpha_{i1}$·GDP·AlF_4^- or $G\alpha_{i1}$·GTPγS analytes yielded robust binding to KB-1753, whereas $G\alpha_{i1}$·GDP exhibited no detectable interaction (Figure 1B). To assess the affinity of these interactions, dissociation constants (K_D values) were obtained by saturation binding using a previously described technique (*20*, *21*). As shown in Figure 1C, $G\alpha_{i1}$ in both the transition state (GDP·AlF_4^-) and activated state (GTPγS) interacts with KB-1753 with a low micromolar affinity. KB-1753 bound with the highest affinity to $G\alpha_{i2}$·GDP·AlF_4^-, nearly 10-fold better than the affinity for either $G\alpha_{i1}$ or $G\alpha_{i3}$ (Figure 1C). No appreciable affinity was detected for the GDP-bound conformation of any of these $G\alpha_i$ subunits, confirming the results of the original phage selection (*10*). A chimeric Gα subunit that closely mimics transducin ("αT*" in which the corresponding region from $G\alpha_{i1}$ was inserted between

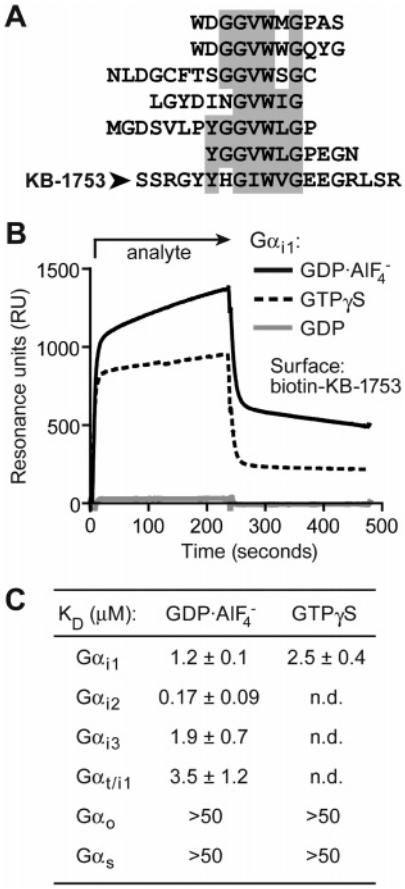

C

K_D (μM):	GDP·AlF_4^-	GTPγS
$Gα_{i1}$	1.2 ± 0.1	2.5 ± 0.4
$Gα_{i2}$	0.17 ± 0.09	n.d.
$Gα_{i3}$	1.9 ± 0.7	n.d.
$Gα_{t/i1}$	3.5 ± 1.2	n.d.
$Gα_o$	>50	>50
$Gα_s$	>50	>50

FIGURE 1: Selective binding of KB-1753 to Gα subunits as measured by surface plasmon resonance (SPR). (A) Sequences of seven peptides, including KB-1753, with a shared sequence (gray) isolated by phage display based on selective binding to immobilized $Gα_{i1}$·GTPγS (*10*). (B) $Gα_{i1}$ protein ("analyte", 10 μM), in each of three nucleotide-bound states as indicated, was injected over immobilized, biotinylated KB-1753 peptide. Nonspecific binding (~200 RU) to a control peptide surface was subtracted from each curve. (C) The indicated Gα subunits, including a chimera between $Gα_{transducin}$ and $Gα_{i1}$ ("$Gα_{t/i1}$"), were separately injected at increasing concentrations (from 0.01 to 50 μM) over immobilized KB-1753 to determine dissociation constants (K_D) for each interaction pair as obtained by saturation binding analysis (*20*, *21*). No binding (K_D > 1000 μM) was seen with any Gα in the GDP-bound state. A K_D of >50 μM denotes interactions with minimal binding responses observed only at saturating concentrations of Gα greater than 50 μM. n.d., not determined.

residues 215 and 294 of $Gα_t$, herein denoted $Gα_{t/i1}$) (*36*) also interacted with KB-1753 in a nucleotide-dependent manner. Interestingly, no detectable affinity was observed for the closely related $Gα_{oA}$ subunit or the more divergent G-protein, $Gα_s$ (Figure 1C).

Overall Structure of the $Gα_{i1}$·GDP·AlF_4^-−KB-1753 Complex. To understand the molecular details of the nucleotide-dependent interaction of KB-1753 with Gα, we determined the structure of KB-1753 bound to $Gα_{i1}$·GDP·AlF_4^- by X-ray diffraction crystallography (Table 1). The conformation of Gα·GDP·AlF_4^- closely resembles that of Gα·GTPγS (*37*, *38*), and AlF_4^- addition activates Gα signaling in vitro (*39*). The overall structure of $Gα_{i1}$ consists of two principal lobes: a Ras-like domain similar to the monomeric GTPase fold and an additional all-helical domain (*11*); the guanine nucleotide binding pocket lies between these two domains. The planar anion AlF_4^-, GDP, and Mg^{2+} are all found in the $Gα_{i1}$−KB-1753 structure as predicted (Figure 2A). Three flexible switch regions, responsible for the conformational changes involved in the guanine nucleotide cycle (*11*), aid in the binding of AlF_4^- and Mg^{2+} (Figure 2A).

Table 1: Data Collection and Refinement Statistics

data collection[a]	
space group	$P3_221$
no. of molecules per asymmetric unit	2
unit cell dimensions	
a, *b*, *c* (Å)	103.13, 103.13, 206.99
α, β, γ (deg)	90, 90, 120
wavelength (Å)	1.1
resolution (Å)	50−2.8 (2.9−2.8)
linear *R*-factor[b]	0.093 (0.416)
square *R*-factor[c]	0.065 (0.330)
mean I/σ[d]	23.1 (2.7)
completeness (%)	94.1 (61.0)
redundancy	6.4 (4.5)
refinement	
resolution (Å)	50−2.8 (2.82−2.8)
no. of reflections (working set/test set)	25452/2824
R_{work}/R_{free} (%)[e]	27.9/30.7
no. of non-hydrogen atoms	
protein	5090
GDP/AlF/Mg	56/10/2
water	30
root-mean-square deviation	
bonds (Å)	0.01
angles (deg)	1.22
average *B*-factor	51.4
Ramachandran plot (%)	
allowed region	98.9
generously allowed region	1.1
disallowed region	0.0

[a] Native data set collected at Brookhaven National Laboratory synchrotron X-ray source on beamline x29. Numbers in parentheses pertain to the highest-resolution shell. [b] Linear *R*-factor = $\sum(|I - \langle I\rangle|)/\sum(I)$. [c] Square *R*-factor = $\sum(|I - \langle I\rangle|)^2/\sum(I)^2$. [d] $\langle I/\sigma I\rangle$, mean signal-to-noise ratio, where *I* is the integrated intensity of a measured reflection and σI is the estimated error in measurement. [e] $R_{work} = \sum[|F_p - F_{p(calc)}|]/\sum F_p$, where F_p and $F_{p(calc)}$ are the observed and calculated structure factor amplitudes, respectively. R_{free} is calculated similarly using test set reflections never used during refinement.

Two nearly identical $Gα_{i1}$−KB-1753 dimers exist in the asymmetric unit with a rmsd of 0.64 Å. Residues Arg-3−Glu-13 of the KB-1753 peptide (S_1SRGYYHGIWVG-EEGRLSR_{19}) were sufficiently ordered to confidently model them on the basis of electron density (Figure 2B,C). KB-1753 binds within the Ras-like domain of $Gα_{i1}$ in a highly conserved hydrophobic cleft formed by the α2 (switch II) and α3 helices (Figure 2). This cleft represents the proposed effector-binding site for $Gα_{i1}$ (*40*) and suggests that KB-1753 binds in an "effector-like" mode to activated-state Gα (see below). Notably, binding of KB-1753 does not significantly alter the conformation of $Gα_{i1}$ as the overall rmsd between bound and unbound structures was calculated to be 0.81 Å. Hydrophobic residues dominate the $Gα_{i1}$−KB-1753 binding interface, including Ile-9 of KB-1753, which lies buried within the hydrophobic pocket created by $Gα_{i1}$ residues Trp-211 and Phe-215. Conservative replacement of this isoleucine with valine leads to a 5-fold decrease in binding affinity, whereas alanine substitution at Ile-9 (in combination with the critical Trp-10; see below) completely abolishes interaction of KB-1753 with $Gα_{i1}$ (Figure 3B). Additional van der Waals contacts are made between His-7 and Ile-212 within this pocket. Other KB-1753−$Gα_{i1}$ contacts include the following: Val-11−Arg-208, Trp-10−

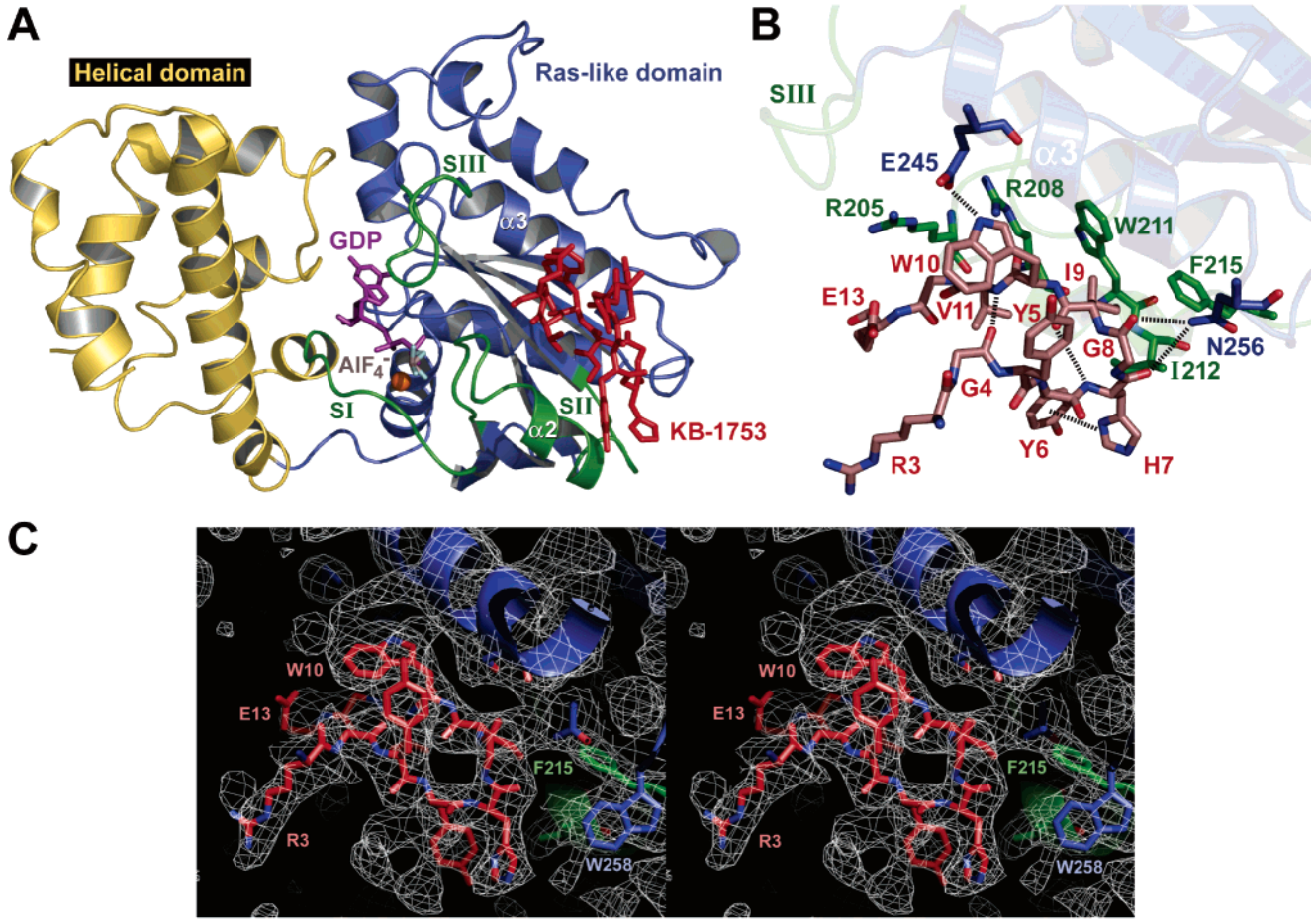

FIGURE 2: Structural features of the $G\alpha_{i1}$−KB-1753 interaction. (A) KB-1753 peptide (red, with side chains) is bound between the α2 (switch II) and α3 helices of the $G\alpha_{i1}$ Ras-like domain (blue; switch regions colored green). No contact is made between KB-1753 and the all-helical domain (yellow), GDP (magenta), AlF_4^- (gray), or magnesium (orange). (B) Representative inter- and intramolecular contacts between $G\alpha_{i1}$ (blue; switch regions colored green) and KB-1753 (tan) residues are shown as black dotted lines. All contacts shown or discussed in the text were selected on the basis of a maximum distance cutoff of 3.7 Å. (C) Stereoview of experimental electron density for KB-1753 bound to $G\alpha_{i1}$, shown as a $2F_o - F_c$ simulated annealing composite omit map generated with a 5% overall model omitted and contoured at 1σ (electron density shown as a white cage). The region highlighted is the entire peptide density (model colored red) lying below the α3 helix (model colored *blue*) and above switch II (model colored green).

Lys-248, Trp-10−Ser-252, His-7−Asn-256, and Gly-8−Asn-256 (Figures 2B and 3A).

When bound to $G\alpha_{i1}$, KB-1753 assumes a hairpin secondary structure centered about residues Tyr-6 and His-7, with several stabilizing intramolecular contacts aiding the adoption of this hairpin (e.g., Figure 2B). The position of the imidazole nitrogen of His-7 raises the possibility of a cation−π interaction with Tyr-6 at the hinge of the hairpin loop. Mutation of this histidine results in a 7-fold reduction in binding affinity ("H7F", Figure 3C). Other intramolecular contacts within the bound conformation of KB-1753 include the following: Gly-4−Val-11, Gly-4−Gly-12, Tyr-5−Trp-10, Tyr-6−Ile-9, and Tyr-6−Val-11 (Figures 2B and 3A). Figure 2C illustrates the electron density depicting the confidence of model building of KB-1753 and its interaction with $G\alpha_{i1}$.

Molecular Basis of Nucleotide-Dependent Interaction. Binding of an activating nucleotide such as GTP, GTPγS, or GDP·AlF_4^- to Gα induces specific structural changes in the three switch regions. The conformations of these switch regions are very similar in the Gα·GDP·AlF_4^- and Gα·GTPγS forms (*11*), explaining the ability of KB-1753 to bind these two conformations equipotently. In these active conformations, Arg-208 in switch II makes a critical contact with Glu-245 of the α3 helix, just beyond switch III, which helps stabilize the switch II conformation (*37*, *38*). Interestingly, the indole nitrogen of Trp-10 in KB-1753 exploits this interaction and makes contacts with both Arg-208 and Glu-245 (Figure 2B). These interactions may thus partially contribute to the selective nature of binding of KB-1753 to activated Gα, as switch II is entirely disordered in the structure of Gα·GDP likely due to a lack of stabilization with switch III (*11*). Indeed, this conserved glutamate residue makes contacts with effectors in the structures of $G\alpha_t$−PDEγ, $G\alpha_{13}$−p115-RhoGEF, and $G\alpha_q$−GRK2 dimers, although the contributing effector residues are not tryptophan as seen here with KB-1753 (*6*). However, the exact degree to which this interaction aids in the nucleotide selectivity of KB-1753 cannot be inferred as Trp-10 may play other critical roles in the Gα−KB-1753 interaction, such as stabilization of the peptide conformation.

The hydrophobic binding pocket created by Trp-211 and Phe-215 likely also contributes to the nucleotide selectivity of KB-1753. The overall architecture of this pocket perfectly accommodates Ile-9 of KB-1753. A highly conservative replacement of Ile-9 with valine, lacking a single methyl

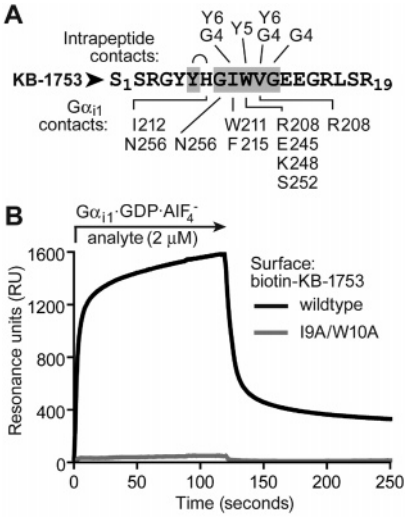

C

KB-1753:	$G\alpha_{i1}$: GDP·AlF_4^-	GDP
wildtype	1.0 ± 0.3	>1000
I9A/W10A	>1000	>1000
I9V	5.2 ± 1.2	>1000
H7F	7.0 ± 2.0	>1000
Y6S/H7F	16.1 ± 3.0	>1000

FIGURE 3: Effects of amino acid substitutions on KB-1753 binding affinity. (A) Summary of intrapeptide and $G\alpha_{i1}$ contacts made by KB-1753 peptide residues. (B) N-Terminally biotinylated KB-1753 peptides, either with the wild-type sequence or mutated (Ile-9 and Trp-10 replaced with alanine), were immobilized on separate streptavidin-coated flow cells, and 2 μM $G\alpha_{i1}$·GDP·AlF_4^- protein (analyte) was injected over both surfaces. Nonspecific binding to a control peptide was subtracted from each curve. (C) Dissociation constants (K_D in micromolar) for the interaction between $G\alpha_{i1}$, in the indicated nucleotide state, and wild-type or mutant KB-1753 peptides immobilized on SPR surfaces. Other parameters are given in Figure 1C.

extension, results in a loss of binding affinity ("I9V", Figure 3C). Furthermore, given the inherent flexibility of switch II in the GDP-bound state (*11*), the integrity of this pocket would be compromised in the inactive conformation. Our recent structural analysis of $G\alpha_{i1}$ bound to a GDP-selective peptide, KB-752, revealed a similar mode of interaction with the Trp-211−Phe-215 pocket (*10*). In the case of KB-752, however, a tryptophan from the peptide was perfectly accommodated by the Trp-211−Phe-215 hydrophobic pocket only in the inactive conformation, given that active conformations sterically clash with the larger tryptophan side chain (*10*). These results underscore the critical involvement of the hydrophobic pocket formed from the α2 and α3 helices in binding these regulatory peptides and dictating their nucleotide selectivities.

KB-1753 Blocks Gα−Effector Interaction. The binding site for KB-1753 on $G\alpha_{i1}$ lies in the putative effector-binding region. Mutational analyses implicate this region as the binding site on $G\alpha_{i1}$ for adenylyl cyclase (*40*). Moreover, $G\alpha_s$−adenylyl cyclase and $G\alpha_t$−PDEγ crystal structures have established the α2−α3 pocket, along with the α2−β4 loop, as the effector binding site for these G-protein subunits (*3*, *4*). As $G\alpha_t$ and $G\alpha_{i1}$ are members of the same Gα subfamily, we focused on the $G\alpha_t$−PDEγ interaction to show that KB-1753 binds to the Gα effector-binding site and could

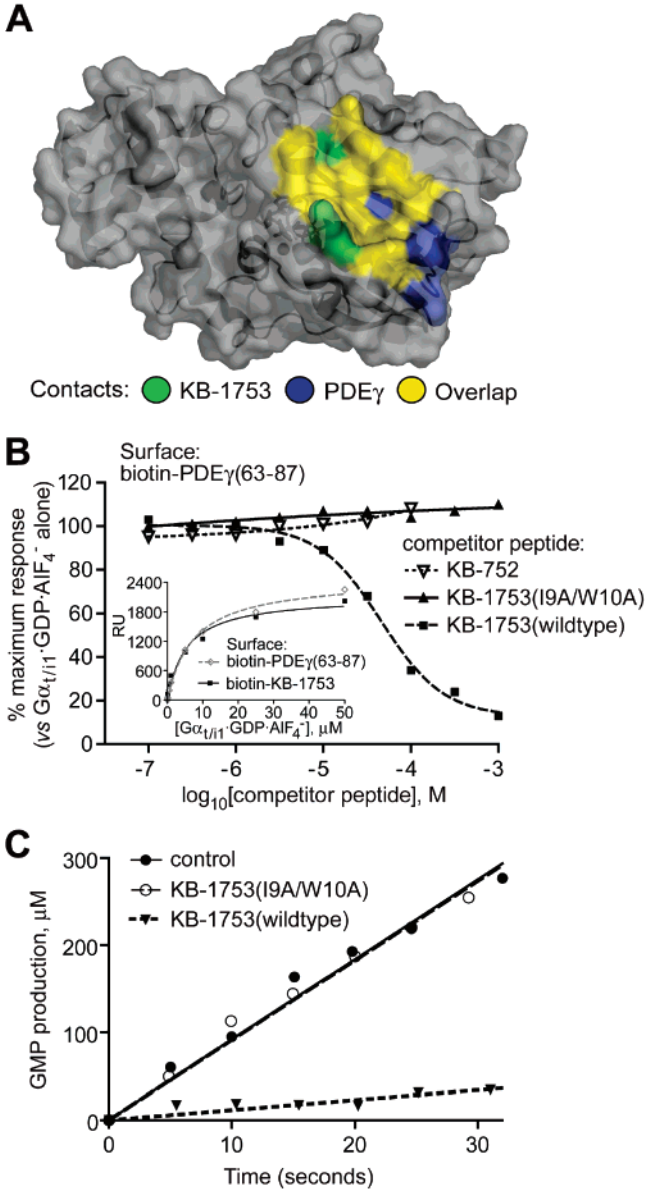

FIGURE 4: KB-1753 acts as an effector antagonist. (A) Surface rendering of $G\alpha_{i1}$·GDP·AlF_4^- (gray) with contact points highlighted for KB-1753 alone (green), contact points highlighted for PDEγ alone (blue), or contact points shared between both interactors (yellow). (B) Wild-type KB-1753 competes with PDEγ for binding to Gα, but not the I9A/W10A mutant peptide or the $G\alpha_{i1}$·GDP-selective peptide KB-752. AlF_4^--activated $G\alpha_{t/i1}$ protein (8.5 μM) was preincubated with the indicated concentrations of competitor peptide prior to injection over a streptavidin SPR surface bearing biotinylated PDEγ(63−87). The inset shows SPR surfaces coated with either biotinylated KB-1753 or PDEγ peptide bind with equivalent affinity to the $G\alpha_{t/i1}$ chimera bound to GDP and AlF_4^-. (C) Rates of cGMP hydrolysis to GMP by transducin-activated PDE6 (0.05 μM) in the absence (control) or presence of 20 μM wild-type or mutant KB-1753 peptides were calculated from linear fits of the data: control, 9.2 μM GMP produced per second; wild-type KB-1753, 1.1 μM GMP produced per second; and I9A/W10A mutant KB-1753, 9.1 μM GMP produced per second. The data were taken from one of three similar experiments.

thus serve as a unique effector antagonist. The $G\alpha_{i1}$−KB-1753 and $G\alpha_t$−PDEγ structures indicate similar modes of Gα interaction between these two peptides (Figure 4A). We first demonstrated using SPR that a soluble $G\alpha_{t/i1}$ chimera [containing $G\alpha_{i1}$ sequence from residue 215 (end of helix α2) through 294 (start of helix α4); ref *36*] could bind both

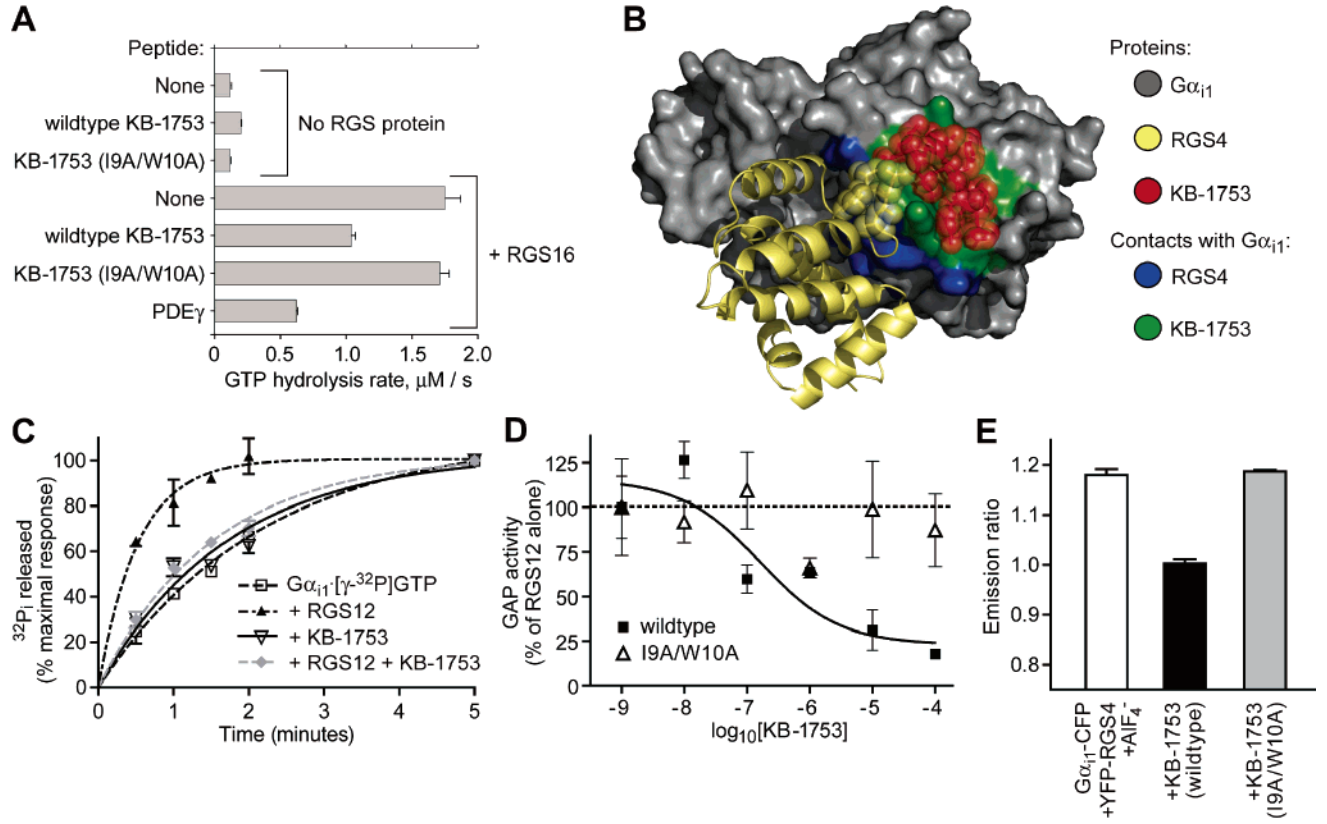

FIGURE 5: KB-1753 interferes with the RGS domain−Gα interaction and RGS-mediated GAP activity. (A) Steady-state rates of GTP hydrolysis by rhodopsin-activated transducin (1 μM) were measured in the absence or presence of 1 μM RGS16 protein, 25 μM PDEγ-(63−87), and/or 20 μM wild-type or mutant KB-1753 peptide, as indicated. GTP hydrolysis rates were determined from linear fits of reaction time courses; the data are averaged from two similar experiments with error bars representing the standard error of the mean. (B) Surface rendering of $G\alpha_{i1}$·GDP·AlF_4^- (gray) bound to RGS4 (cream; derived from PDB entry 1AGR) and overlaid with a space-filling representation of KB-1753 (red). Note that contacts made to $G\alpha_{i1}$·GDP·AlF_4^- by RGS4 (blue) and by KB-1753 (green) are not overlapping, yet steric hindrance is predicted between bound KB-1753 and the α5−α6 loop of RGS4 (amino acids 120−123 shown in space-filling mode). (C) Single-turnover GTP hydrolysis assay using [γ-^{32}P]GTP-labeled $G\alpha_{i1}$ (0.1 μM) in the absence or presence of 0.1 μM RGS12 RGS domain, 1 μM KB-1753, or both. (D) Dose dependence of wild-type KB-1753-mediated inhibition of RGS12 RGS domain GAP activity, as measured in single-turnover GTPase assays performed as described for panel B. I9A/W10A mutant KB-1753 shows no inhibitory activity. (E) Effect of 2 μM KB-1753 peptide (wild type or I9A/W10A mutant) on AlF_4^--dependent FRET between 0.2 μM $G\alpha_{i1}$−CFP and 0.2 μM YFP−RGS4 fusion proteins; FRET was quantified by the emission ratio (525 nm/474 nm), representing the ratio of YFP emission to CFP emission maxima upon excitation at 433 nm.

KB-1753 and a peptide comprising residues 63−87 of PDEγ (Figure 4B inset). We next tested whether KB-1753 and PDEγ exhibit mutually exclusive binding to $G\alpha_{t/i1}$. As expected, preincubation of $G\alpha_{t/i1}$ with free KB-1753 inhibited (in a dose-dependent manner) binding of $G\alpha_{t/i1}$·GDP·AlF_4^- to biotinylated KB-1753 immobilized on the SPR biosensor (data not shown). Preincubation with KB-1753 also abrogated binding of $G\alpha_{t/i1}$·GDP·AlF_4^- to a biotinylated PDEγ peptide surface (Figure 4B). These results establish that KB-1753 competes for binding of the effector (PDEγ) to $G\alpha_{t/i1}$, suggesting that KB-1753 could serve as an effector antagonist in the transducin−PDE signaling pathway.

We thus tested whether KB-1753 could perturb interaction of wild-type $G\alpha_t$ with, and signaling to, cGMP phosphodiesterase (PDE6) by reconstituting these proteins with photoreceptor membranes containing light-activatable rhodopsin, the receptor upstream of transducin. As part of the phototransduction signaling pathway, $G\alpha_t$·GTP activates PDE6 by binding directly to PDEγ and releasing the inhibitory constraint which PDEγ imposes on the α and β catalytic subunits of PDE6 (*41*). We tested whether KB-1753 could impair PDE6 activation by $G\alpha_t$·GTP by measuring the steady-state rate of cGMP degradation to GMP. Rhodopsin-activated transducin was observed to stimulate degradation of cGMP in reconstituted ROS membranes (Figure 4C). KB-1753, but not the I9A/W10A substituted peptide, nearly abolished the stimulation of PDE6 cGMP hydrolysis activity (Figure 4C). Together, the results from SPR competition binding and PDE6 activity assays confirm the ability of KB-1753 to interdict GPCR-mediated signaling through activated G-proteins to effector enzyme activity and suggest that KB-1753 could serve as a novel tool for antagonizing these signaling pathways.

KB-1753 Interferes with RGS Protein GAP Activity. We also reasoned that, by binding to the transition-state mimetic form of Gα (Gα·GDP·AlF_4^-), KB-1753 may alter the intrinsic and/or RGS protein-stimulated GTPase activity of $G\alpha_t$ and $G\alpha_{i1}$. The experiments conducted with wild-type $G\alpha_t$ reconstituted with photoreceptor membranes revealed the presence of both effects (Figure 5A). Addition of KB-1753 caused a nearly 2-fold increase in the basal rate of $G\alpha_t$ GTPase activity. This activity may arise from stabilization of switch II by KB-1753 in a conformation suitable for the catalytic Gln-204 of Gα to more efficiently participate in GTP hydrolysis. Addition of KB-1753 also caused an ~40% reversal of GTPase acceleration by an RGS protein, RGS16,

previously shown to act on $G\alpha_t$ (*42*). Neither effect was observed with the control I9A/W10A substituted peptide. The partial inhibition of RGS16 GAP activity by KB-1753 was very similar to the well-documented partial inhibition caused by PDEγ (lowest bar in Figure 5A; see refs *43* and *44* for original observation).

Comparing the Gα−KB-1753 and Gα−RGS4 structures reveals no significant alterations in the overall Gα backbone (rmsd of 0.68 Å) or of the critical catalytic residues (R178, T181, and Q204). However, space-filling models of KB-1753 and RGS4 indicate that, although KB-1753 binds to the effector-binding region of Gα, which is exclusive from the RGS protein-binding interface (*5*, *6*), the C-terminus of KB-1753 could sterically hinder the access of the RGS protein to its Gα binding site (Figure 5B). KB-1753 significantly blocked the GAP activity of RGS12 on $G\alpha_{i1}$ (Figure 5C,D), suggesting that KB-1753 interferes with RGS protein binding. We also observed a small peptide-dependent acceleration of basal $G\alpha_{i1}$ GTPase activity (Figure 5C), although, unlike in the case of wild-type $G\alpha_t$ (Figure 5A), this effect was not statistically significant. Using a fluorescence resonance energy transfer (FRET)-based assay for Gα−RGS protein interactions (*34*), we confirmed that KB-1753 is able to block the direct interaction between RGS4 and $G\alpha_{i1}$ (Figure 5E). Thus, KB-1753 serves as a novel peptide inhibitor of $G\alpha_{i1}$−RGS protein interaction and RGS-mediated GAP activity in vitro.

A Fusion of KB-1753 with the Yellow Fluorescent Protein Serves as a Sensor for Activated Gα. Fluorescent biosensors have become instrumental for investigating protein−protein interactions as well as protein activation in real time and visualizing the spatiotemporal aspects of signal transduction in live cells (*45*, *46*). The ability of KB-1753 to bind only activated Gα makes it a potentially useful tool for developing novel biosensors for G-protein activation. In an initial test of this hypothesis, we employed FRET between chromatic variants of the *Aequoria victoria* green fluorescent protein in which excitation of a donor cyan fluorescent protein (CFP) in turn excites an acceptor yellow fluorescent protein (YFP) when these variants are within defined distance constraints (~50 Å) (*47*). We subcloned the KB-1753 peptide sequence N-terminal to YFP (KB-1753−YFP) to serve as a FRET acceptor for CFP-modified $G\alpha_{i1}$ (Figure 5B; ref *34*). KB-1753−YFP underwent a robust FRET response with CFP−$G\alpha_{i1}$, selectively in the presence of aluminum tetrafluoride (Figure 6A,B) and with an affinity of ~750 nM (Figure 6C). Incubation of CFP−$G\alpha_{i1}$ with excess unmodified KB-1753 (but not the I9A/W10A mutant) blocked the FRET response (Figure 6B). These results validate KB-1753−YFP as a bona fide FRET partner for detecting the activated conformation of CFP-tagged $G\alpha_{i1}$, a form of KB-1753 that could be directly applied to in vivo settings (*45*, *46*).

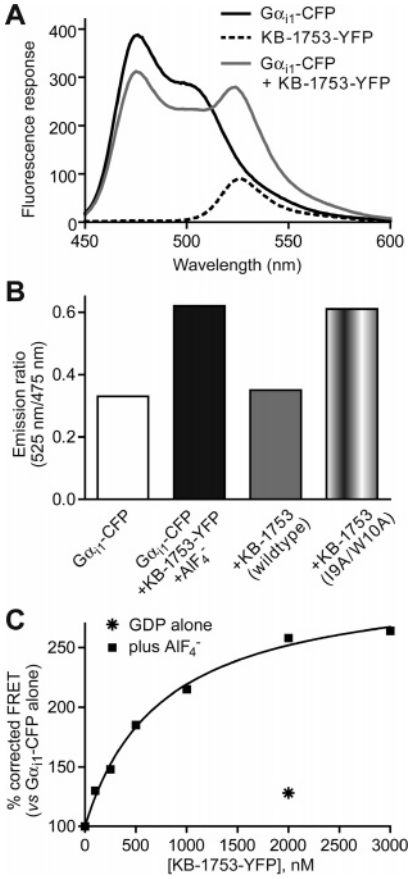

FIGURE 6: KB-1753−yellow fluorescent protein fusion acts as a sensor for activated $G\alpha_{i1}$. (A) $G\alpha_{i1}$−CFP (200 nM) and/or KB-1753−YFP (500 nM) fusion proteins were added to cuvettes containing assay buffer [10 mM Tris (pH 7.5), 1 mM EDTA, 10 mM $MgCl_2$, 150 mM NaCl, 10 μM GDP, 30 μM $AlCl_3$, and 10 mM NaF; the latter two reagents forming the Gα activator aluminum tetrafluoride] and allowed to incubate for 60 s before emission scans (from 450 to 600 nm) were taken using an excitation wavelength of 433 nm at 20 nm/minute and slit widths of 5 nm. Data shown are uncorrected fluorescence measurements under each indicated condition. (B) FRET between 0.5 μM KB-1753−YFP and 0.2 μM $G\alpha_{i1}$·GDP·AlF_4^-−CFP fusion proteins is inhibited by preincubation of Gα with 2 μM wild-type KB-1753 peptide; preincubation with 2 μM I9A/W10A mutant was observed to have no effect on the emission ratio. (C) Dose- and nucleotide-state-dependent FRET between 0.2 μM $G\alpha_{i1}$−CFP and indicated concentrations of KB-1753−YFP fusion protein. Data are expressed as "corrected FRET" obtained by subtracting the emission of KB-1753−YFP alone from each FRET condition. The apparent dissociation constant obtained for the KB-1753−YFP/$G\alpha_{i1}$·GDP·AlF_4^-−CFP interaction was 0.76 ± 0.08 μM (best fit ± standard error).

DISCUSSION

The structural basis of G-protein regulation resides in subtle conformational changes in three critical switch regions of the Gα subunit (*11*). When GDP is released from the inactive, G$\beta\gamma$-complexed conformation, Gα binds GTP and adopts the active conformation capable of regulating effector molecules. Regulatory proteins (such as RGS proteins and GoLoco proteins) exploit these distinct nucleotide-dependent conformations of Gα for their binding and modulation of the nucleotide cycle (*7*, *8*, *48*). Here, we have described a peptide, KB-1753, capable of interacting with specific Gα subunits solely in active conformations. The crystal structure of this peptide bound to $G\alpha_{i1}$·GDP·AlF_4^- reveals an "effector-like" mode of binding, relying on the specific conformation of the switch II helix. KB-1753 serves as an effector antagonist as well as an inhibitor of RGS protein activity. These qualities make KB-1753 an attractive new tool for studying G-protein signaling. The development of biosensors for activated Gα using KB-1753 should open new avenues for both in vitro assay design and real-time in vivo imaging of Gα activation.

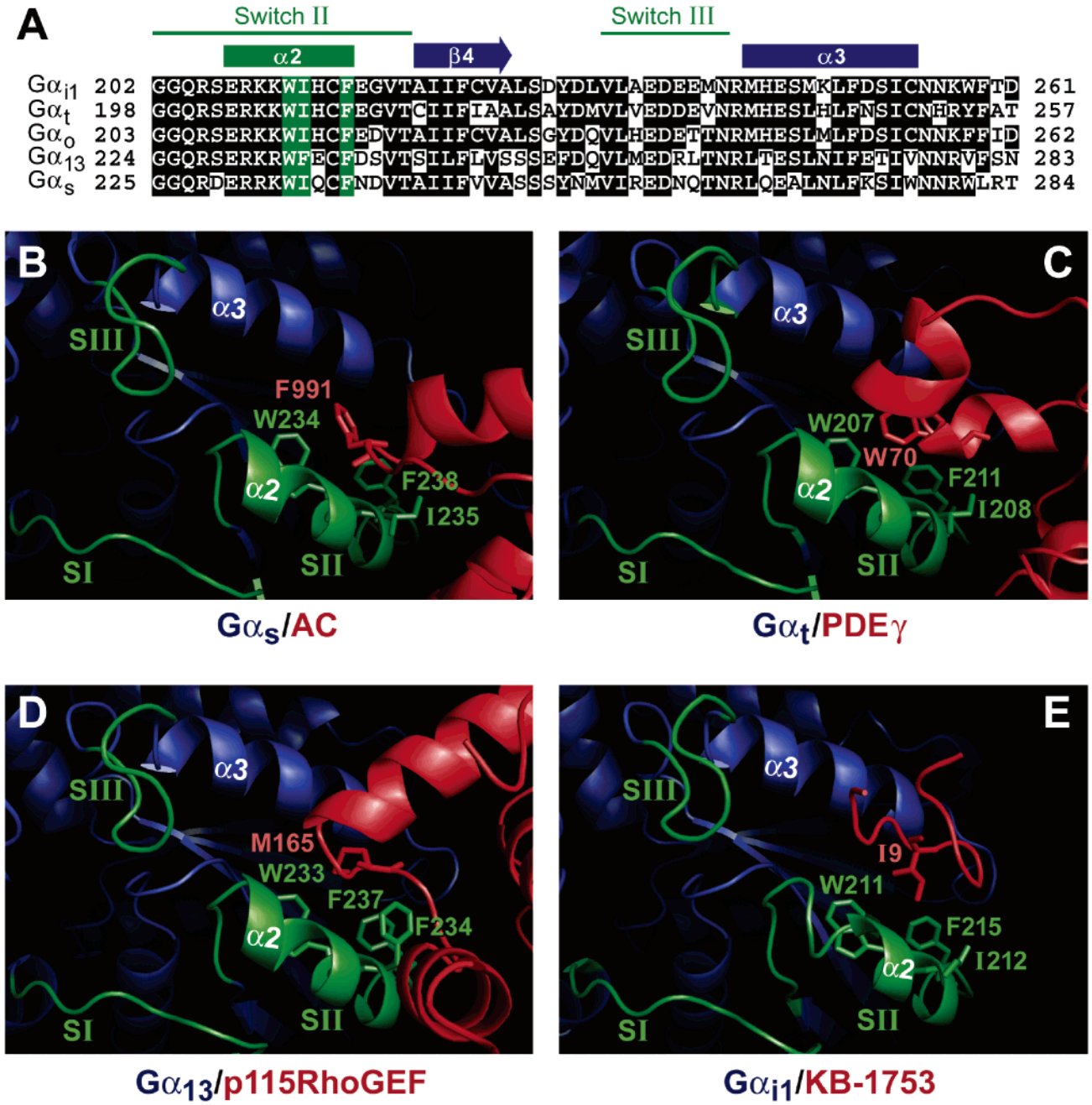

FIGURE 7: Conserved structural features of engagement of Gα by effectors and by KB-1753. (A) Multiple-sequence alignment derived from Clustal-X (*59*) of human $G\alpha_{i1}$ (GenBank entry AAM12619), bovine $G\alpha_t$ (SwissProt entry P04695), human $G\alpha_o$ (SwissProt entry P09471), human $G\alpha_{13}$ (GenBank entry NP_006563), and bovine $G\alpha_s$ (SwissProt entry P04896) sequences, highlighting locations of switch II and switch III, as well as conservation of three hydrophobic residues involved in effector engagement (green boxes). Burial of a key hydrophobic residue of an effector (red) within a conserved hydrophobic cleft between switch II (α2) and α3 helices of activated Gα (blue; switch regions colored green) is apparent in the crystal structures of $G\alpha_s$·GTPγS bound to the second cytoplasmic domain of type II adenylyl cyclase (AC) [B (*3*)], $G\alpha_t$·GDP·AlF_4^- bound to the γ subunit of cGMP phosphodiesterase (PDEγ) [C (*4*)], the N-terminal RGS domain of the RhoA guanine nucleotide exchange factor p115RhoGEF interacting with GDP·AlF_4^--bound $G\alpha_{13/i-5}$, a chimeric Gα subunit based on $G\alpha_{i1}$ but containing the three switch regions and the helical domain of $G\alpha_{13}$ [D (*5*)], and $G\alpha_{i1}$·GDP·AlF_4^- bound to the KB-1753 peptide [E (this study)].

Currently, available Gα−effector structures include those of $G\alpha_s$−adenylyl cyclase, $G\alpha_q$−GRK2, $G\alpha_{13}$−p115RhoGEF, and $G\alpha_t$−PDEγ−RGS9 complexes (*3*−*6*). Although $G\alpha_t$ belongs to the $G\alpha_i$ family, currently no specific structural analysis of a $G\alpha_{i1-3}$−effector complex exists. Thus, the $G\alpha_{i1}$−KB-1753 complex represents the first structural glimpse of $G\alpha_{i1}$ engaged in an effector-like recognition mode, albeit with a nonphysiological target. On the basis of the $G\alpha_s$−adenylyl cyclase structure and the pseudosymmetry of the C1 and C2 cytosolic lobes of adenylyl cyclase (*3*), mutational analysis has identified residues within the C1 lobe of type V adenylyl cyclase (ACV) critical to $G\alpha_{i1}$ regulation (*49*). Specifically, these critical C1 lobe residues reside in the α1−α2 and α3−β4 segments of ACV, with the latter segment proposed to bind within the switch II−α3 cleft of $G\alpha_i$, the binding site for KB-1753. However, no significant sequence similarity was observed between KB-1753 and the α3−β4 loop of ACV. A sequence of S**L**VRE**M**TGVNV within the

ACV $\alpha3-\beta4$ loop has been implicated in binding the switch II$-\alpha3$ cleft of $G\alpha_i$; bold, underlined residues indicate particular positions that, when mutated, result in loss of $G\alpha_i$-mediated inhibition (*49*). Aside from a general hydrophobic character in this region of ACV that may complement the hydrophobic cleft in Gα, no significant homology with KB-1753 exists. Thus, KB-1753 appears to be a unique sequence that exploits the same effector-binding region of $G\alpha_{i1}$ and suggests that diverse primary sequences in effectors may recognize a similar binding motif within Gα. Indeed, the switch II$-\alpha3$ cleft utilized by effectors is highly conserved among Gα subfamilies (Figure 7) (*3*−*6*); therefore, diversity within effectors, in either primary sequence or tertiary structure, must compensate for the common Gα binding groove to allow for signaling specificity (*6*). This difficulty in defining Gα−effector specificity based on the conserved nature of structurally defined interactions has been previously discussed (*6*). Another possibility is that additional regions of Gα define effector specificity by complementing the conserved interactions within the switch II$-\alpha3$ cleft. For example, regions within the $\alpha4-\beta6$ loop of $G\alpha_{i2}$ (specifically ^{314}RKDTKE^{319}) have been implicated in the interaction with adenylyl cyclase (*40*). However, KB-1753 makes no contact within this region of Gα. Also, the $\alpha2-\beta4$ and $\alpha3-\beta5$ regions of Gα have been implicated in effector binding; however, with the exception of $G\alpha_s$, these sequences are also highly conserved (*6*). The ability of KB-1753 to inhibit binding and signaling of wild-type transducin to PDE6, an effector with which KB-1753 also lacks significant sequence similarity, signifies its effector-like mode of binding to $G\alpha_{i1}$ and further underscores the sequence diversity in effectors available for Gα subunit recognition.

KB-1753 is a potentially attractive new tool for studying G-protein signaling. If modified to allow cell penetration (e.g., ref *50*), KB-1753 could effectively block $G\alpha_i$·GTP−effector signaling while preserving receptor−heterotrimer coupling and $G\beta\gamma$-mediated signaling, unlike pertussis toxin which permanently impairs $G\alpha_i\beta\gamma$ coupling and signaling via ADP ribosylation (*51*) or of siRNA-mediated *Gnai* transcript silencing which can result in compensatory up-regulation of other $G\alpha_{i/o}$ family members (*52*). The selective interaction of KB-1753 with $G\alpha_i$ subunits over $G\alpha_o$ (Figure 1B) would provide another advantage in interrogating GPCR coupling specificity over pertussis toxin, the latter acting nonspecifically on all $G\alpha_{i/o}$ subfamily members except $G\alpha_z$ (*53*). The ability of KB-1753 to block RGS protein binding and resultant GAP activity highlights yet another potential usefulness of this novel peptide.

Biosensors capable of visualizing the spatiotemporal aspects of protein activation and protein−protein interactions have become indispensable tools for studying signal transduction events within the context of live cells (*47*, *54*). Several studies using CFP/YFP FRET and related techniques have investigated GPCR signaling dynamics (*55*−*58*). Studies aimed at examining heterotrimer activation have used designs wherein activation leads to a reduction in the magnitude of the FRET response due to the dissociation of a Gα−CFP and $G\beta\gamma$−YFP coupled pair (for example, ref *57*). Although innovative and informative, these studies are limited by their reliance on a loss of FRET response which presents specific technical challenges (such as correcting for photobleaching artifacts) and limits the ability to track the spatiotemporal aspects of Gα signaling once activated. Our KB-1753−YFP species, however, presents an attractive alternative design that produces an increase in the level of the FRET response following Gα activation (Figure 6) and should allow resolution of the spatiotemporal dynamics of activated Gα signaling. Moreover, as Gα becomes deactivated, a loss of FRET response would be expected, given that KB-1753−YFP binds selectively to only the activated form. Thus, a FRET-based approach with KB-1753−YFP could report both the activation and deactivation dynamics of Gα signaling, potentially improving the resolution of previous studies. We are now avidly working toward this goal.

ACKNOWLEDGMENT

We thank Dr. C. McCudden for $G\alpha_{i2}$, $G\alpha_{i3}$, and RGS12 constructs, Dr. D. Doyle (SGC Oxford, Oxford, U.K.) for the RGS16 plasmid, and Drs. R. Pereira and R. Cerione (Cornell University, Ithaca, NY) for the αT* plasmid. Special thanks to the data collection facilities of the National Synchrotron Light Source, Brookhaven National Laboratory, U.S. Department of Energy, Division of Materials Sciences and Division of Chemical Sciences (Contract DE-AC02-98CH10886).

REFERENCES

1. McCudden, C. R., Hains, M. D., Kimple, R. J., Siderovski, D. P., and Willard, F. S. (2005) G-Protein signaling: Back to the future, *Cell. Mol. Life Sci. 62*, 551−77.
2. Wettschureck, N., and Offermanns, S. (2005) Mammalian G proteins and their cell type specific functions, *Physiol. Rev. 85*, 1159−204.
3. Tesmer, J. J., Sunahara, R. K., Gilman, A. G., and Sprang, S. R. (1997) Crystal structure of the catalytic domains of adenylyl cyclase in a complex with Gsα·GTPγS, *Science 278*, 1907−16.
4. Slep, K. C., Kercher, M. A., He, W., Cowan, C. W., Wensel, T. G., and Sigler, P. B. (2001) Structural determinants for regulation of phosphodiesterase by a G protein at 2.0 Å, *Nature 409*, 1071−7.
5. Chen, Z., Singer, W. D., Sternweis, P. C., and Sprang, S. R. (2005) Structure of the p115RhoGEF rgRGS domain-Gα13/i1 chimera complex suggests convergent evolution of a GTPase activator, *Nat. Struct. Mol. Biol. 12*, 191−7.
6. Tesmer, V. M., Kawano, T., Shankaranarayanan, A., Kozasa, T., and Tesmer, J. J. (2005) Snapshot of activated G proteins at the membrane: The Gαq-GRK2-Gβγ complex, *Science 310*, 1686−90.
7. Ross, E. M., and Wilkie, T. M. (2000) GTPase-activating proteins for heterotrimeric G proteins: Regulators of G protein signaling (RGS) and RGS-like proteins, *Annu. Rev. Biochem. 69*, 795−827.
8. Siderovski, D. P., and Willard, F. S. (2005) The GAPs, GEFs, and GDIs of heterotrimeric G-protein α subunits, *Int. J. Biol. Sci. 1*, 51−66.
9. Johnston, C. A., Ramer, J. K., Blaesius, R., Fredericks, Z., Watts, V. J., and Siderovski, D. P. (2005) A bifunctional Gαi/Gαs modulatory peptide that attenuates adenylyl cyclase activity, *FEBS Lett. 579*, 5746−50.
10. Johnston, C. A., Willard, F. S., Jezyk, M. R., Fredericks, Z., Bodor, E. T., Jones, M. B., Blaesius, R., Watts, V. J., Harden, T. K., Sondek, J., Ramer, J. K., and Siderovski, D. P. (2005) Structure of $G\alpha_{i1}$ bound to a GDP-selective peptide provides insight into guanine nucleotide exchange, *Structure 13*, 1069−80.
11. Sprang, S. R. (1997) G protein mechanisms: Insights from structural analysis, *Annu. Rev. Biochem. 66*, 639−78.
12. Hamm, H. E. (2001) How activated receptors couple to G proteins, *Proc. Natl. Acad. Sci. U.S.A. 98*, 4819−21.
13. Meng, E. C., and Bourne, H. R. (2001) Receptor activation: What does the rhodopsin structure tell us? *Trends Pharmacol. Sci. 22*, 587−93.
14. Rondard, P., Iiri, T., Srinivasan, S., Meng, E., Fujita, T., and Bourne, H. R. (2001) Mutant G protein α subunit activated by Gβγ: A model for receptor activation? *Proc. Natl. Acad. Sci. U.S.A. 98*, 6150−5.

15. Davis, T. L., Bonacci, T. M., Sprang, S. R., and Smrcka, A. V. (2005) Structural and molecular characterization of a preferred protein interaction surface on G protein $\beta\gamma$ subunits, *Biochemistry 44*, 10593−604.
16. Hessling, J., Lohse, M. J., and Klotz, K. N. (2003) Peptide G protein agonists from a phage display library, *Biochem. Pharmacol. 65*, 961−7.
17. Ja, W. W., and Roberts, R. W. (2004) In vitro selection of state-specific peptide modulators of G protein signaling using mRNA display, *Biochemistry 43*, 9265−75.
18. Scott, J. K., Huang, S. F., Gangadhar, B. P., Samoriski, G. M., Clapp, P., Gross, R. A., Taussig, R., and Smrcka, A. V. (2001) Evidence that a protein-protein interaction 'hot spot' on heterotrimeric G protein $\beta\gamma$ subunits is used for recognition of a subclass of effectors, *EMBO J. 20*, 767−76.
19. Stols, L., Gu, M., Dieckman, L., Raffen, R., Collart, F. R., and Donnelly, M. I. (2002) A new vector for high-throughput, ligation-independent cloning encoding a tobacco etch virus protease cleavage site, *Protein Expression Purif. 25*, 8−15.
20. Kimple, R. J., Willard, F. S., Hains, M. D., Jones, M. B., Nweke, G. K., and Siderovski, D. P. (2004) Guanine nucleotide dissociation inhibitor activity of the triple GoLoco motif protein G18: Alanine-to-aspartate mutation restores function to an inactive second GoLoco motif, *Biochem. J. 378*, 801−8.
21. McCudden, C. R., Willard, F. S., Kimple, R. J., Johnston, C. A., Hains, M. D., Jones, M. B., and Siderovski, D. P. (2005) Gα selectivity and inhibitor function of the multiple GoLoco motif protein GPSM2/LGN, *Biochim. Biophys. Acta 1745*, 254−64.
22. Snow, B. E., Antonio, L., Suggs, S., and Siderovski, D. P. (1998) Cloning of a retinally abundant regulator of G-protein signaling (RGS-r/RGS16): Genomic structure and chromosomal localization of the human gene, *Gene 206*, 247−53.
23. Arshavsky, V. Y., Dumke, C. L., Zhu, Y., Artemyev, N. O., Skiba, N. P., Hamm, H. E., and Bownds, M. D. (1994) Regulation of transducin GTPase activity in bovine rod outer segments, *J. Biol. Chem. 269*, 19882−7.
24. Nekrasova, E. R., Berman, D. M., Rustandi, R. R., Hamm, H. E., Gilman, A. G., and Arshavsky, V. Y. (1997) Activation of transducin guanosine triphosphatase by two proteins of the RGS family, *Biochemistry 36*, 7638−43.
25. Snow, B. E., Brothers, G. M., and Siderovski, D. P. (2002) Molecular cloning of regulators of G-protein signaling family members and characterization of binding specificity of RGS12 PDZ domain, *Methods Enzymol. 344*, 740−61.
26. Otwinowski, Z., and Minor, W. (1997) Processing of X-ray diffraction data collected in oscillation mode, *Methods Enzymol. 276*, 307−26.
27. Navaza, J. (2001) Implementation of molecular replacement in AMoRe, *Acta Crystallogr. D57*, 1367−72.
28. Jones, T. A., Zou, J. Y., Cowan, S. W., and Kjeldgaard, M. (1991) Improved methods for building protein models in electron density maps and the location of errors in these models, *Acta Crystallogr. A47* (Part 2), 110−9.
29. Brunger, A. T., Adams, P. D., Clore, G. M., DeLano, W. L., Gros, P., Grosse-Kunstleve, R. W., Jiang, J. S., Kuszewski, J., Nilges, M., Pannu, N. S., Read, R. J., Rice, L. M., Simonson, T., and Warren, G. L. (1998) Crystallography & NMR system: A new software suite for macromolecular structure determination, *Acta Crystallogr. D54* (Part 5), 905−21.
30. Artemyev, N. O., Arshavsky, V. Y., and Cote, R. H. (1998) Photoreceptor phosphodiesterase: Interaction of inhibitory γ subunit and cyclic GMP with specific binding sites on catalytic subunits, *Methods 14*, 93−104.
31. Ross, E. M. (2002) Quantitative assays for GTPase-activating proteins, *Methods Enzymol. 344*, 601−17.
32. Martemyanov, K. A., and Arshavsky, V. Y. (2004) Kinetic approaches to study the function of RGS9 isoforms, *Methods Enzymol. 390*, 196−209.
33. Skiba, N. P., Hopp, J. A., and Arshavsky, V. Y. (2000) The effector enzyme regulates the duration of G protein signaling in vertebrate photoreceptors by increasing the affinity between transducin and RGS protein, *J. Biol. Chem. 275*, 32716−20.
34. Willard, F. S., Kimple, R. J., Kimple, A. J., Johnston, C. A., and Siderovski, D. P. (2004) Fluorescence-based assays for RGS box function, *Methods Enzymol. 389*, 56−71.
35. Gasteiger, E., Jung, E., and Bairoch, A. (2001) SWISS-PROT: Connecting biomolecular knowledge via a protein database, *Curr. Issues Mol. Biol. 3*, 47−55.
36. Pereira, R., and Cerione, R. A. (2005) A switch 3 point mutation in the α subunit of transducin yields a unique dominant-negative inhibitor, *J. Biol. Chem. 280*, 35696−703.
37. Coleman, D. E., Berghuis, A. M., Lee, E., Linder, M. E., Gilman, A. G., and Sprang, S. R. (1994) Structures of active conformations of Giα1 and the mechanism of GTP hydrolysis, *Science 265*, 1405−12.
38. Sondek, J., Lambright, D. G., Noel, J. P., Hamm, H. E., and Sigler, P. B. (1994) GTPase mechanism of Gproteins from the 1.7-Å crystal structure of transducin α-GDP-AIF-4, *Nature 372*, 276−9.
39. Sternweis, P. C., and Gilman, A. G. (1982) Aluminum: A requirement for activation of the regulatory component of adenylate cyclase by fluoride, *Proc. Natl. Acad. Sci. U.S.A. 79*, 4888−91.
40. Grishina, G., and Berlot, C. H. (1997) Identification of common and distinct residues involved in the interaction of αi2 and αs with adenylyl cyclase, *J. Biol. Chem. 272*, 20619−26.
41. Arshavsky, V. Y., Lamb, T. D., and Pugh, E. N., Jr. (2002) G proteins and phototransduction, *Annu. Rev. Physiol. 64*, 153−87.
42. Chen, C. K., Wieland, T., and Simon, M. I. (1996) RGS-r, a retinal specific RGS protein, binds an intermediate conformation of transducin and enhances recycling, *Proc. Natl. Acad. Sci. U.S.A. 93*, 12885−9.
43. Natochin, M., Granovsky, A. E., and Artemyev, N. O. (1997) Regulation of transducin GTPase activity by human retinal RGS, *J. Biol. Chem. 272*, 17444−9.
44. Wieland, T., Chen, C. K., and Simon, M. I. (1997) The retinal specific protein RGS-r competes with the γ subunit of cGMP phosphodiesterase for the α subunit of transducin and facilitates signal termination, *J. Biol. Chem. 272*, 8853−6.
45. Hahn, K., and Toutchkine, A. (2002) Live-cell fluorescent biosensors for activated signaling proteins, *Curr. Opin. Cell Biol. 14*, 167−72.
46. Johnston, C. A., and Siderovski, D. P. (2006) Resolving G protein-coupled receptor signaling mechanics in vivo using fluorescent biosensors, *Cellscience Rev. 2*, 16−24.
47. Zhang, J., Campbell, R. E., Ting, A. Y., and Tsien, R. Y. (2002) Creating new fluorescent probes for cell biology, *Nat. Rev. Mol. Cell Biol. 3*, 906−18.
48. Willard, F. S., Kimple, R. J., and Siderovski, D. P. (2004) Return of the GDI: The GoLoco motif in cell division, *Annu. Rev. Biochem. 73*, 925−51.
49. Dessauer, C. W., Tesmer, J. J., Sprang, S. R., and Gilman, A. G. (1998) Identification of a Giα binding site on type V adenylyl cyclase, *J. Biol. Chem. 273*, 25831−9.
50. Lindsay, M. A. (2002) Peptide-mediated cell delivery: Application in protein target validation, *Curr. Opin. Pharmacol. 2*, 587−94.
51. Katada, T., Bokoch, G. M., Smigel, M. D., Ui, M., and Gilman, A. G. (1984) The inhibitory guanine nucleotide-binding regulatory component of adenylate cyclase. Subunit dissociation and the inhibition of adenylate cyclase in S49 lymphoma cyc- and wild type membranes, *J. Biol. Chem. 259*, 3586−95.
52. Krumins, A. M., and Gilman, A. G. (2006) Targeted knockdown of G protein subunits selectively prevents receptor-mediated modulation of effectors and reveals complex changes in non-targeted signaling proteins, *J. Biol. Chem.* (in press).
53. Fields, T. A., and Casey, P. J. (1997) Signalling functions and biochemical properties of pertussis toxin-resistant G-proteins, *Biochem. J. 321* (Part 3), 561−71.
54. Chamberlain, C., and Hahn, K. M. (2000) Watching proteins in the wild: Fluorescence methods to study protein dynamics in living cells, *Traffic 1*, 755−62.
55. Bunemann, M., Frank, M., and Lohse, M. J. (2003) Gi protein activation in intact cells involves subunit rearrangement rather than dissociation, *Proc. Natl. Acad. Sci. U.S.A. 100*, 16077−82.
56. Hein, P., Frank, M., Hoffmann, C., Lohse, M. J., and Bunemann, M. (2005) Dynamics of receptor/G protein coupling in living cells, *EMBO J. 24*, 4106−14.
57. Janetopoulos, C., Jin, T., and Devreotes, P. (2001) Receptor-mediated activation of heterotrimeric G-proteins in living cells, *Science 291*, 2408−11.
58. Vilardaga, J. P., Bunemann, M., Krasel, C., Castro, M., and Lohse, M. J. (2003) Measurement of the millisecond activation switch of G protein-coupled receptors in living cells, *Nat. Biotechnol. 21*, 807−12.
59. Aiyar, A. (2000) The use of CLUSTAL W and CLUSTAL X for multiple sequence alignment, *Methods Mol. Biol. 132*, 221−41.

BI0613832